

Electronic State of a Conducting Single Molecule Magnet Based on Mn-salen Type and Ni-Dithiolene Complexes

Kazuya Kubo,^{*,†,‡} Takuya Shiga,^{†,§} Takashi Yamamoto,^{||} Akiko Tajima,[⊥] Taro Moriwaki,[#] Yuka Ikemoto,[#] Masahiro Yamashita,^{*,†} Elisa Sessini,[∇] Maria Laura Mercuri,[∇] Paola Deplano,[∇] Yasuhiro Nakazawa,^{||} and Reizo Kato[⊥]

[†]Department of Chemistry, Graduate School of Science, Tohoku University, 6-3, Aramaki-Aza-Aoba, Aoba-Ku, Sendai, 980-8578 Miyagi, Japan

[‡]Research Institute for Electronic Science, Hokkaido University, Kita 20 Nishi 10, Kita-ku, Sapporo 001-0020, Japan

[§]Graduate School of Pure and Applied Science, University of Tsukuba, Tennodai 1-1-1, Tsukuba, 305-8571 Ibaraki, Japan

^{||}Department of Chemistry, Graduate school of Science, Osaka University, 1-1, Machikaneyama, Toyonaka, 560-0043 Osaka, Japan

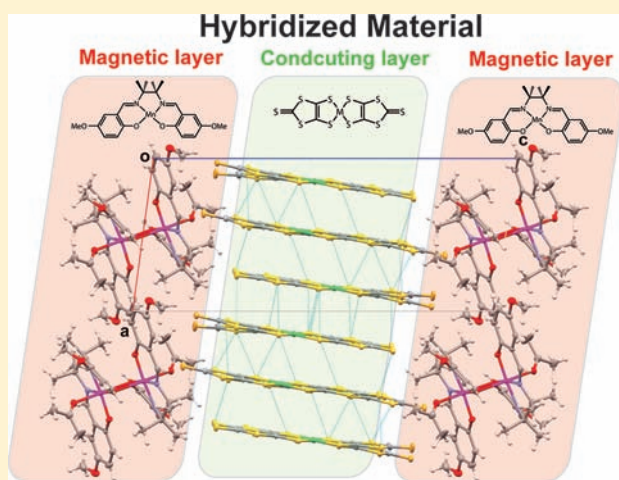
[⊥]RIKEN, 2-1, Hirosawa, Wako-shi, Saitama 351-0198, Japan

[#]JASRI/SPring-8, 1-1-1, Kouto, Sayo-cho, Sayo-gun, Hyogo 679-5198, Japan

[∇]Dipartimento di Chimica Inorganica ed Analitica, Università di Cagliari, Cittadella di Monserrato, I-09042 Monserrato, Cagliari, Italy

S Supporting Information

ABSTRACT: The electrochemical oxidation of an acetone solution containing $[\text{Mn}^{\text{III}}(5\text{-MeOsaltmen})(\text{H}_2\text{O})_2](\text{PF}_6)_2$ ($5\text{-MeOsaltmen}^{2-} = N,N'$ -(1,1,2,2-tetramethylethylene)bis(5-methoxy-salicylideneimine)) and $(\text{NBu}_4)[\text{Ni}(\text{dmit})_2]$ ($\text{dmit}^{2-} = 2\text{-thioxo-1,3-dithiole-4,5-dithiolate}$) afforded a hybrid material, $[\text{Mn}(5\text{-MeOsaltmen})(\text{acetone})]_2[\text{Ni}(\text{dmit})_2]_6$ (**1**), in which $[\text{Mn}_2]^{2+}$ single-molecule magnets (SMMs) with an $S_T = 4$ ground state and $[\text{Ni}(\text{dmit})_2]^{n-}$ molecules in a charge-ordered state ($n = 0$ or 1) are assembled in a layer-by-layer structure. Compound **1** crystallizes in the triclinic space group $P\bar{1}$ with an inversion center at the midpoint of the $\text{Mn} \cdots \text{Mn}$ dimer. The $[\text{Mn}_2]^{2+}$ unit has a typical nonplanar Mn(III) dimeric core and is structurally consistent with previously reported $[\text{Mn}_2]$ SMMs. The six $[\text{Ni}(\text{dmit})_2]^{n-}$ ($n = 0$ or 1) units have a square-planar coordination geometry, and the charge ordering among them was assigned on the basis of $\nu(\text{C}=\text{C})$ in IR reflectance spectra (1386, 1356, 1327, and 1296 cm^{-1}). The $[\text{Mn}_2]^{2+}$ SMM and $[\text{Ni}(\text{dmit})_2]^{n-}$ units aggregate independently to form hybrid frames. Electronic conductivity measurements revealed that **1** behaved as a semiconductor ($\rho_{\text{rt}} = 2.1 \times 10^{-1} \Omega \cdot \text{cm}^{-1}$, $E_a = 97 \text{ meV}$) at ambient pressure and as an insulator at 1.7 GPa ($\rho_{1.7\text{GPa}} = 4.5 \Omega \cdot \text{cm}^{-1}$, $E_a = 76 \text{ meV}$). Magnetic measurements indicated that the $[\text{Mn}_2]^{2+}$ units in **1** behaved as $S_T = 4$ SMMs at low temperatures.



1. INTRODUCTION

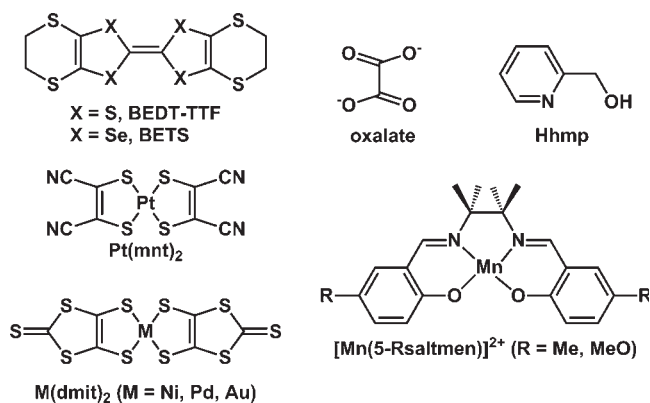
In the field of molecular material science, the design of multifunctional materials, such as magnetic/conducting bifunctional materials, has been intensively studied.¹ A general method for designing such materials involves the hybridization of individual parts with magnetic and conducting frames via molecular self-assembly. Coronado et al. reported the first hybridized materials consisting of ferromagnetic layers of $[\text{Mn}^{\text{II}}\text{Cr}^{\text{III}}(\text{ox})_3]^-$ ($\text{ox} = \text{oxalate}^{2-}$) and metallic layers of bis(ethylenedithio)-tetrathiafulvalene (BEDT-TTF) or bis(ethylenedithio)tetraselenafulvalene (BETS) molecules.² Many hybridized materials, such as paramagnet/superconductor, ferromagnet/superconductor, and ferromagnet/metal, have been prepared.^{2–4}

These compounds are hybridized materials based on molecular conductors and classical magnets. However, material scientists have been most interested in the correlation between relaxing local spins and conducting π electrons in superparamagnetic/conducting hybrid materials from the viewpoint of developing quantum spintronics. Single-molecule magnet (SMM) properties are attributed to intrinsic characteristics of the individual molecule, that is, high-spin ground state (S_T) and uniaxial anisotropy, which is indicated by a large negative D and a small E in relation to the following Hamiltonian anisotropy term: $H = DS_T^2 + E(S_{Tx}^2 - S_{Ty}^2)$. The large D and small E values

Received: April 24, 2011

Published: September 02, 2011

cause a finite energy barrier (Δ) between spin-up and spin-down m_s states ($m_s = \pm S_T$) expressed as $|D|S_T^2$ for integer values of S_T



and $|D|(S_T^2 - 1/4)$ for half-integer values of S_T . Therefore, SMMs exhibit slow relaxation of the magnetization and quantum phenomena, such as quantum tunneling of the magnetization (QTM) between quantum states of m_s , which can be tuned via Δ or decoherent energy levels of the quantum states.^{5–11} We have been interested in the correlations between relaxing local spins and conducting π electrons in superparamagnetic/conducting hybrid materials. From recent results of studies on SMM-based supramolecular oligomers and networked compounds,^{12–18} the inter-SMM interactions have a small effect on both SMMs via the conducting electrons.

Miyasaka et al. have suggested that SMMs can be used as magnetic building blocks to prepare molecular assemblies.¹⁹ In developing their work on crystal engineering based on SMM or anisotropic molecule building blocks, their group has designed new classes of magnetic materials, including single-chain magnets (SCMs) and multidimensional SMM networks, which they call nanodot networks.^{15,16,20} Recently, they reported the first example of hybrid materials with both SMMs and molecular conducting layers.²¹ This material involves a Coulomb pair of a cationic SMM, double-cuboidal mixed valence $[\text{Mn}_4]^{4+}$ clusters of $[\text{Mn}^{\text{II}}_2\text{Mn}^{\text{III}}_2(\text{hmp})_6(\text{MeCN})_2(\text{H}_2\text{O})_4](\text{ClO}_4)_4$ (hmp = 2-hydroxymethylpyridinate[−], MeCN = acetonitrile),²² and an anionic molecular conductor, $(\text{Bu}_4\text{N})[\text{Pt}(\text{mnt})_2]$ (mnt^{2−} = maleonitriledithiolate(2−)).²³ Electrochemical oxidation of a solution containing both starting building blocks yielded a hybrid compound containing six $[\text{Pt}(\text{mnt})_2]^{n−}$, where n = noninteger valence, per $[\text{Mn}_4]^{4+}$ SMM core, which behaves as an SMM/semiconductor. However, diffusion of the starting materials led simply to a counterion exchange reaction, affording an assembly with four $[\text{Pt}(\text{mnt})_2]^{n−}$ molecules per $[\text{Mn}_4]^{4+}$ SMM, which acts as a SMM/insulator. Another type of SMM/semiconductor or insulator, $[\text{Mn}(\text{5-MeOsaltmen})(\text{solvent})]_2[\text{Ni}(\text{dmit})_2]_7 \cdot 4(\text{solvent})$ (solvent = acetone or MeCN; dmit^{2−} = 2-thioxo-1,3-dithiole-4,5-dithiolate) and $[\text{Mn}(\text{5-Rsaltmen})\{\text{M}(\text{dmit})_2\}]_2$ (R = Me, MeO; M = Ni, Au), has been prepared in order to improve the conduction properties^{24,25} because $[\text{M}(\text{dmit})_2]^{n−}$ has better electronic conductivity than $[\text{Pt}(\text{mnt})_2]^{n−}$ does due to a smaller HOMO–LUMO gap and because it prefers to interact with other molecules in three dimension.²⁶

Another method to change the physical properties of hybridized materials is to change the ratio of the cation and anion. The ratio and the molecular arrangements of the hybrid materials affect their physical properties.²⁷ Previously, we reported the new hybrid material $[\text{Mn}(\text{5-MeOsaltmen})(\text{acetone})]_2[\text{Ni}(\text{dmit})_2]_6$

(1).²⁸ Although this material is a SMM/semiconductor, it has a peculiar electronic state. In this paper, the electronic state of **1** is discussed on the bases of crystal structure, electrical conductivity, magnetic susceptibility, infrared reflectance spectra, and band calculations.

2. EXPERIMENTAL SECTION

2.1. Preparation and Crystal Structure Determination of $[\text{Mn}(\text{5-MeOsaltmen})(\text{acetone})]_2[\text{Ni}(\text{dmit})_2]_6$ (**1**).

Single crystals of radical cation salt **1** were prepared by electrochemical crystallization of an acetone solution of $[\text{Mn}(\text{5-MeOsaltmen})(\text{H}_2\text{O})][\text{PF}_6]$ and $(\text{Bu}_4\text{N})[\text{Ni}(\text{dmit})_2]$, as previously reported.^{28–30} The chemical formula of the complex was determined on the basis of elemental and X-ray crystal structural analyses. Crystallographic data for **1**: chemical formula, $\text{C}_{43}\text{H}_{32}\text{Mn}_2\text{Ni}_3\text{O}_5\text{S}_{30}$; crystal system, triclinic; space group, $P\bar{1}$; $a = 10.115(2)$ Å; $b = 12.998(3)$ Å; $c = 25.374(6)$ Å; $\alpha = 97.322(3)^\circ$, $\beta = 97.076(3)^\circ$; $\gamma = 98.119(3)^\circ$; $Z = 2$.²⁸

2.2. Band Calculations.

Intermolecular overlap integrals (S) between the frontier orbitals were determined by using extended Hückel molecular orbital (MO) calculations. The semiempirical parameters for the Slater-type atomic orbitals were taken from the literature.³¹ Transfer integrals, t , were calculated by using the equation $t = -10S$.

2.3. Magnetic Susceptibility Measurements.

The magnetic susceptibility of **1** (15.7 mg) was measured on a Quantum Design SQUID magnetometer (MPMS-XL) in the temperature and direct current (dc) field ranges of 1.8–300 K and -7 to $+7$ T, respectively. Alternating current (ac) susceptibilities were determined in the frequency range of 1–1488 Hz with an ac field amplitude of 3 Oe. A polycrystalline sample of **1** embedded in liquid paraffin was used for the measurements. Experimental data were corrected for the sample holder, including the liquid paraffin, and for the diamagnetic contribution calculated from Pascal constants.³²

2.4. Electrical Resistivity Measurements.

The temperature dependence of the electrical resistivity of **1** was measured by using a standard four-probe method at ambient pressure. Gold wires (15 μm diameter) were attached to the crystal with carbon paste. High-pressure resistivity measurements on **1** were performed in the range of 0.2–1.7 GPa using a clamp-type piston-cylinder high pressure cell.³³

2.5. IR Reflectance Spectroscopy.

Polarized reflectance spectra were acquired in the Spring-8 BL43IR beamline with a microscope. The spectral resolution was 4 cm^{-1} . The light polarization was set parallel ($\parallel a$) and perpendicular ($\perp b^*$) to the stacking directions in the two-dimensional (2-D) sheets or almost parallel to the c axis, which is almost parallel to the long axis of $[\text{Ni}(\text{dmit})_2]$.

3. RESULTS AND DISCUSSION

3.1. Structural Features of **1**.

Figure 1 shows the structural features of **1**.²⁸ The asymmetric unit has one crystallographically independent $[\text{Mn}(\text{5-MeOsaltmen})(\text{acetone})]^{+}$ and three $[\text{Ni}(\text{dmit})_2]$ molecules. There are inversion centers at the midpoint of the $\text{Mn} \cdots \text{Mn}$ vector of the cationic $[\text{Mn}(\text{5-MeOsaltmen})(\text{acetone})]_2^{2+}$ dimers. The dimer unit has a typical nonplanar Mn(III) dimeric core and is structurally consistent with other reported $[\text{Mn}]_2$ SMMs.³⁴ The nickel ions in the anions have square planar coordination geometries similar to those of other d^8 metal ion complexes. Bond lengths and angles of $[\text{Ni}(\text{dmit})_2]$ are in the same range found in other 1:3 radical anion salts of $[\text{Ni}(\text{dmit})_2]$, such as $[\text{Co}(\eta\text{-C}_5\text{H}_5)_2][\text{Ni}(\text{dmit})_2]_3$,³⁵ $(\text{NBu})_{0.29}\text{Ni}(\text{dmit})_2$,³⁶ $(\text{TPP})[\text{Ni}(\text{dmit})_2]_3$ (TPP = tetraphenylphosphonium),³⁷ and $[\text{TSF}][\text{Ni}(\text{dmit})_2]_3$ (TSF = tetraselenafulvalene).³⁸

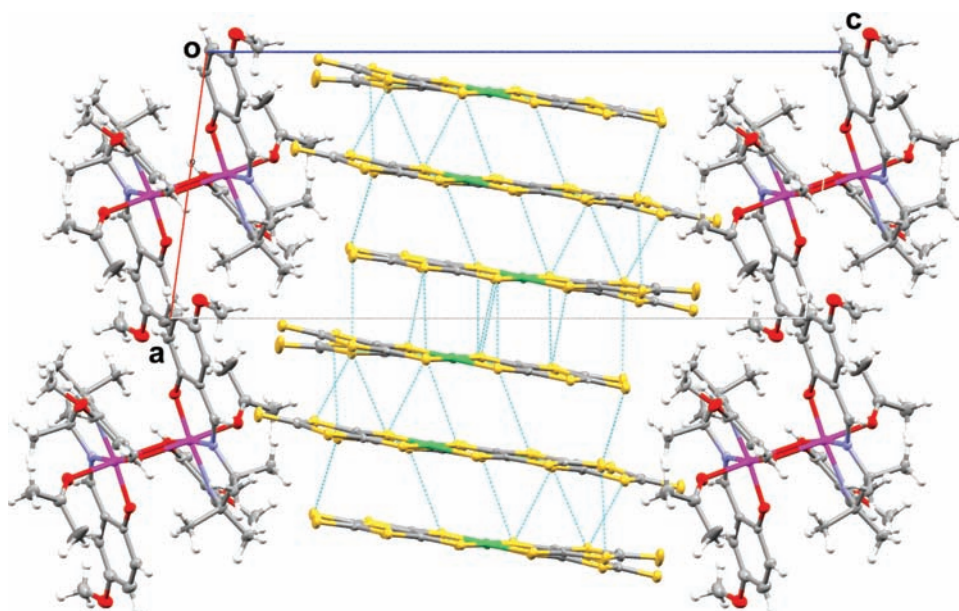


Figure 1. Structural features of **1**. Dashed lines indicate sulfur–sulfur contacts shorter than the sum of the van der Waals radii (3.7 Å).

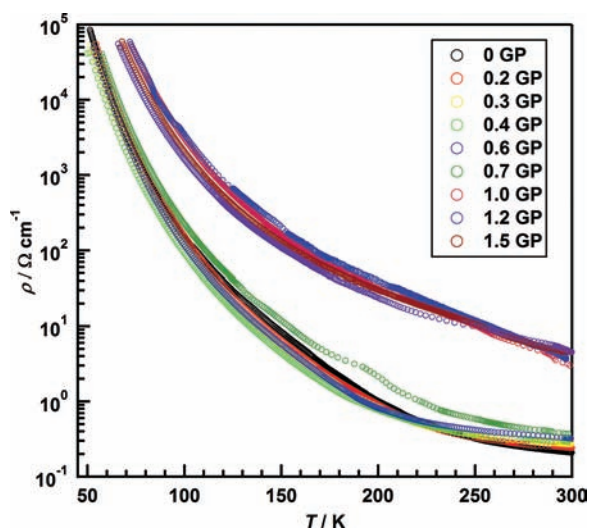


Figure 2. Temperature dependence of the resistivity of **1** from ambient pressure to 1.5 GPa.

In this crystal, the cationic dimers and the anions form layers parallel to the *ab* plane. In the $[\text{Mn}^{\text{III}}]_2^{2+}$ dimer layer, there is no significant interaction between the dimers through π – π contacts as observed in $[\text{Mn}(5\text{-MeOsaltmen})(\text{acetone})]_2[\text{Ni}(\text{dmit})_2]_7 \cdot 4\text{acetone}$ (Figure 4).²⁴ In the anionic layer, a one-dimensional columnar structure is formed by stacks of the three $[\text{Ni}(\text{dmit})_2]$ molecules in the following arrangement, $\cdots [\text{Ni}(1)] - [\text{Ni}(2)] - [\text{Ni}(3)] - [\text{Ni}(3)] - [\text{Ni}(2)] - [\text{Ni}(1)] \cdots$. Intermolecular interactions through sulfur–sulfur contacts (3.546–3.679 Å) shorter than the sum of the van der Waals radii (3.7 Å) between the anionic molecules are present along the stacking direction and the *b* axis. In this salt, three $[\text{Ni}(\text{dmit})_2]$ asymmetric molecules have a total valence of -1 . The electronic state of the $[\text{Ni}(\text{dmit})_2]$ moiety in **1**, which is either a uniform

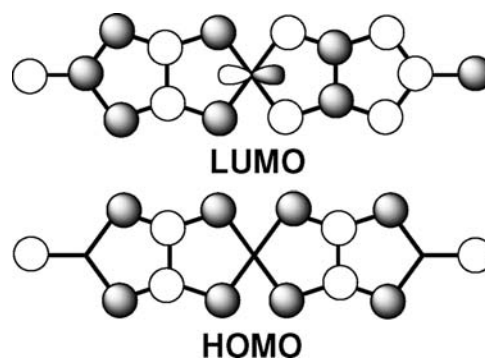


Figure 3. HOMO and LUMO of the neutral state of a $[\text{Ni}(\text{dmit})_2]$ molecule in **1**.

charged trimer state or a charge-ordered state, is discussed later on the basis of IR reflectance spectra.

3.2. Electrical Resistivity. Figure 2 shows temperature dependence of the electrical resistivity of **1** under various pressures. Compound **1** exhibited semiconducting behavior with a small activation energy ($\rho_{\text{rt}} = 2.1 \times 10^{-1} \Omega \cdot \text{cm}^{-1}$, $E_a = 97$ meV) at ambient pressure. Although the activation energy slightly decreased at 1.7 GPa, **1** behaved as an insulator ($\rho_{1.7 \text{ GPa}} = 4.5 \Omega \cdot \text{cm}^{-1}$, $E_a = 76$ meV). The application of pressure controlled the electronic structure by changing the intermolecular interactions, as observed for other molecular conductors.^{26,39–41} The mechanism for this behavior depends on the origin of the insulating state at ambient pressure. The pressure experiments suggest that the band of the insulating state of **1** is 1/6 full. The character of the insulating state of **1** is further discussed on the basis of spectroscopic and magnetic studies. The resistivity curves can be classified into two groups and are discussed in the next section.

3.3. Energy Band Calculation. The energy band structure of **1** was calculated using an extended Hückel MO tight-binding method with the structural data. Figure 3 shows the HOMO and

Table 1. Calculated Overlap Integrals ($S \times 10^3$) between the LUMOs of $[\text{Ni}(\text{dmit})_2]$ of **1**

$S (\times 10^3)$	$S (\times 10^3)$	$S (\times 10^3)$
a1	b1	p1
a2	b2	p2
a3	b3	p3
a4	b4	

LUMO for the anion moiety of **1**. The HOMO and LUMO are characteristic of $M(\text{dmit})_2$ complexes. The HOMO of the $M(\text{dmit})_2$ molecule has b_{1u} symmetry, whereas the LUMO has b_{2g} symmetry. The metal d orbital can mix with the LUMO but cannot with the HOMO due to the symmetry, destabilizing the HOMO and thus causing a small energy gap between the HOMO and LUMO. The side-by-side intermolecular interactions, which lead to the formation of a two-dimensional electronic structure, have a larger contribution from the HOMO than they do from the LUMO. This is because some of overlap integrals (S) for the intermolecular $S \cdots S$ pairs are canceled out due to the b_{2g} symmetry of the LUMO.

The calculated S values between the LUMOs are listed in Table 1 with a schematic drawing of their arrangement in the anion moiety of **1**. On the basis of the LUMO, a quasi-one-dimensional structure is formed because S values within the column (a1–a4) are much larger than those involving the side-by-side interactions (b1–b4 and p1–p3). The calculated energy band structure formed from the LUMOs is shown in Figure S1 (Supporting Information). There are 12 separated narrow bands from the LUMOs (see Table 1). Three of the $[\text{Ni}(\text{dmit})_2]$ molecules in the assembly have one electron, meaning that the band is 1/6 full (red bands in Figure S1). The calculations indicate that **1** is a band insulator.

Applying pressure on organic conductors mainly affects the bandwidth, W , and on-site coulomb repulsion, U . It appeared that there was a greater effect on U when pressure was applied during the resistivity measurements (Figure 2). The resistivity at room temperature rapidly increased when the pressure was

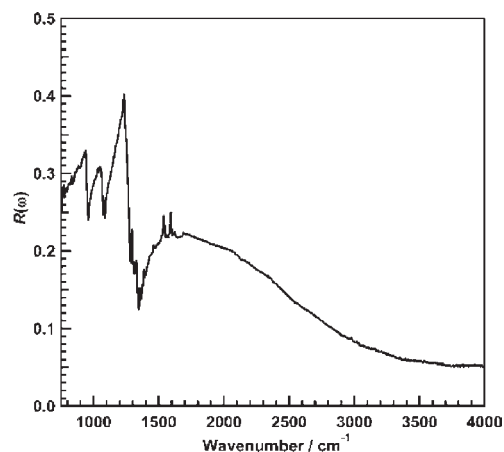


Figure 4. Polarized IR reflectance spectrum of **1** along the a axis at 300 K.

greater than 0.7 GPa. We believe that U increases rapidly above 0.7 GPa. Anisotropic measurements of the resistivity can reveal the origin of the resistivity. However, the measurement is difficult because the crystals of **1** were thin plates.

3.4. IR Spectrum. In order to investigate the electronic structure of **1**, polarized IR reflectance spectra were acquired in the Spring-8 BL43IR beamline. Figure 4 shows a polarized IR reflectance spectrum of **1** polarized along the a axis. The reflectance ($R(\omega)$) spectrum for $E \parallel a$ had two distinct features: a broad maximum around 1800 cm^{-1} with an edge structure below 3000 cm^{-1} and a low-wavenumber portion below 1500 cm^{-1} , showing a few characteristic peaks. The broad maximum was not observed for $E \parallel b$ and $E \parallel c$. These features indicate that **1** is a quasi-one-dimensional semiconductor. The mid-IR peak in the $R(\omega)$ spectrum mainly corresponds to an intermolecular charge transfer (CT) transition typically observed for various molecular conductors with quasi-one-dimensional character.⁴² The two peaks observed at 1591 and 1690 cm^{-1} were attributed to $\nu(\text{C}=\text{N})$ and $\nu(\text{C}=\text{O})$ of the cationic dimer $[\text{Mn}(\text{S-MeOsaltmen})(\text{acetone})_2]^{2+}$.

Figure 5 shows a magnification of the IR spectrum in Figure 4 in the range of $750\text{--}1500 \text{ cm}^{-1}$. In this region, four peaks at 1386 , 1356 , 1327 , and 1296 cm^{-1} , labeled ν_{1_rich} , ν_{2_rich} , ν_{1_poor} , and ν_{2_poor} , where ν_1 and ν_2 are the in-phase and out-of-phase $\text{C}=\text{C}$ stretching modes of $\text{Ni}(\text{dmit})_2$ and “rich” and “poor” denote charge-rich and -poor molecules, respectively, were observed. The four IR peaks are at positions similar to those for other 1:3 $[\text{Ni}(\text{dmit})_2]$ salts.^{35–38} A broad maximum around 1150 cm^{-1} with dips corresponding to $\nu(\text{C}-\text{S})$ (970 cm^{-1}) and $\nu(\text{C}=\text{S})$ (1050 cm^{-1}) stretching modes was assigned to a $\text{C}=\text{C}$ stretching mode. The broad maximum was attributed to an electron-molecular vibrational (e-mv) interaction due to coupling between the CT transition and a $\text{C}=\text{C}$ stretching mode. The electronic state of $[\text{M}(\text{dmit})_2]$ ($\text{M} = \text{Ni}, \text{Pd}$) can be estimated from the peak position of the vibration modes of the molecule because these peaks and the maximum are sensitive to the charge.⁴³ On the basis of the assignment of the vibrational modes of neutral and reduced $[\text{Pd}(\text{dmit})_2]$ reported by Yamamoto et al.,⁴⁴ the four peaks and the maximum in Figure 5 were assigned to a combination of the fundamental $\text{C}=\text{C}$ stretching modes ν_1 and ν_2 of the six $[\text{Ni}(\text{dmit})_2]$ molecules in the symmetric unit of the crystal. Thus, considering the S in the a direction, as described in section 3.3, the symmetric unit

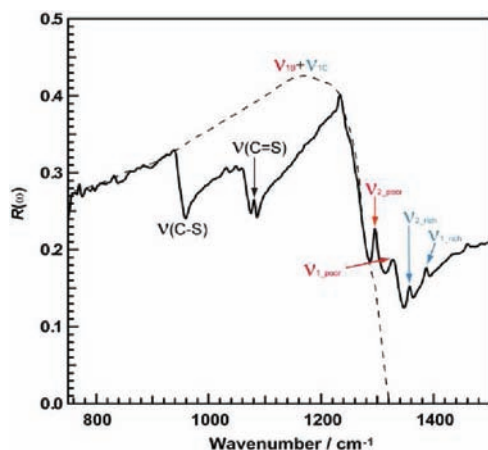


Figure 5. Polarized IR reflectance spectrum of **1** along the *a* axis from 750–1500 cm^{-1} at 300 K.

consists of a tetramer and a dimer: $[-\text{Molecule3}'=\text{Molecule3}-\text{Molecule2}=\text{Molecule1}=\text{Molecule1}'=\text{Molecule2}'-\text{Molecule3}'=]$, where “=” and “-” represent large and small *S* in the *a*-direction, respectively. This symmetric unit consists of two equivalent trimers ($[=\text{Molecule3}-\text{Molecule2}=\text{Molecule1}]=$) and one asymmetric trimer ($[=\text{Molecule1}'=\text{Molecule2}'-\text{Molecule3}'=]$). Combinations of in-phase and out-of-phase *S*'s between two trimers cause three IR-active ν_1 and three Raman-active ν_1 modes. On the other hand, only two ν_2 modes belonging to the charge-poor and -rich molecules should be observed in the IR spectra because the asymmetric ν_2 mode is not involved in the e-mv interaction and is sensitive to the charge of the molecules. Therefore, there should be five C=C stretching modes. In other words, our experimental results are consistent with this argument. Interestingly, the separation in the frequency between ν_{1_rich} and ν_{1_poor} is similar to that between ν_{2_rich} and ν_{2_poor} . This phenomenon indicates that the ν_{1_rich} and ν_{1_poor} modes are less perturbed by the e-mv interaction. In other words, they are charge localized. Thus, this spectrum strongly suggests that the electronic state of the anion moiety is a charge-ordered state. On the other hand, the line width of ν_{1C} is significantly broad as compared to the corresponding mode in the anionic dimer $(\text{Bu}_4\text{N})[\text{Pd}(\text{dmit})_2]$.⁴⁴ This observation suggests that a charge-rich molecule is sandwiched by charge-poor molecules, which favors large coupling with the CT transition. The charge on $[\text{Ni}(\text{dmit})_2]$ can be estimated from the IR spectrum, electrical resistivity, and energy band calculations. From the spectrum, the charge is [neutral]–[monoanion]–[neutral]. In other words, the neutral molecules are Molecule1 and Molecule3, and the anionic one is Molecule2. This charge ordering occurs through weak interactions between the anionic molecules. In the column, there are two neutral molecules, [Molecule1] and [Molecule3]. The side-by-side interactions between anionic [Molecule2] are very weak because transfer integrals *b*2 and *b*4 are 0.21 and -0.0098 . The anions are arranged in quasi-one-dimensional $S = 1/2$ spin chains. The charge-ordered state is supported by the electrical resistivity measurements. Generally, molecular conductors in a charge-ordered state exhibit metallic or superconducting behavior under pressure because the charge-ordered state is broken by pressure.⁴⁵ In this case, however, the anionic molecules do not affect each other due to the arrangement of the molecules and the

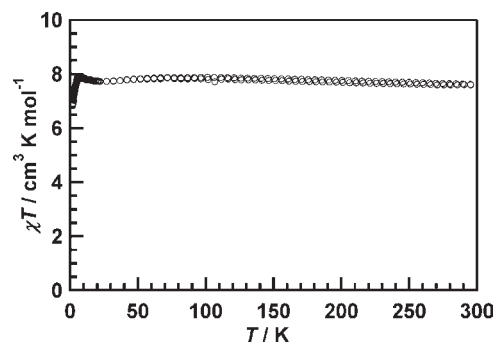


Figure 6. Temperature dependence of χT of **1** measured at 500 Oe.

weak transfer integrals. DC magnetic susceptibility measurements also support this charge-ordered state (see next section).

3.5. Magnetic Susceptibility. **3.5.1. DC Magnetic Susceptibility.** The temperature dependence of DC magnetic susceptibility of a polycrystalline sample of **1** was studied in a 500 Oe field in the temperature range of 1.8–300 K. Figure 6 shows a χT versus *T* plot of **1**. The value of χT slightly increased from $7.60 \text{ cm}^3 \cdot \text{K} \cdot \text{mol}^{-1}$ at 300 K to $7.86 \text{ cm}^3 \cdot \text{K} \cdot \text{mol}^{-1}$ at 70 K and then slightly decreased to $7.74 \text{ cm}^3 \cdot \text{K} \cdot \text{mol}^{-1}$ at 20 K. Ferromagnetic interactions between manganese ions were observed around 8 K. This behavior is quite different from that of isolated $[\text{Mn}_2]^{2+}$ SMMs. The 2:7 salt $[\text{Mn}(\text{S-MeOsaltmen})(\text{acetone})]_2 \cdot [\text{Ni}(\text{dmit})_2]_7 \cdot 4\text{acetone}$, which has a molecular packing similar to **1**, exhibits ferromagnetic behavior, which is typical of isolated $[\text{Mn}^{\text{III}}]^{2+}$ SMMs.²⁴ The χT behavior of the 2:7 salt can be simulated using a Heisenberg dimer model with $S = 2$, taking into account zero field splitting (ZFS) of the Mn(III) ion (D_{Mn}): $H = -2J\hat{S}_{\text{Mn}1}\hat{S}_{\text{Mn}2} + 2D_{\text{Mn}}S_{\text{Mn},z}^2$, where $S_{\text{Mn},z}$ is the *z* component of the $S_{\text{Mn},i}$ spin vectors. In this case, however, the value of χT of **1** at 300 K is large compared to that of the Mn dimer only ($\sim 6.0 \text{ cm}^3 \cdot \text{K} \cdot \text{mol}^{-1}$).⁴⁶ We think that this is due to the contribution of the two $\text{Ni}(\text{dmit})_2$ units with $S = 1/2$ (see previous section). The χT behavior of **1** can be understood by considering complicated interactions, such as the $[\text{Mn}_2]^{2+} \cdots [\text{Mn}_2]^{2+}$, $[\text{Ni}]^{n-} \cdots [\text{Ni}]^{n-}$, and $[\text{Mn}_2]^{2+} \cdots [\text{Ni}]^{n-}$. However, we could not accurately fit the magnetic data for **1**.

3.5.2. ac Magnetic Susceptibilities. The temperature dependence of the ac susceptibilities was first measured in a 3 Oe ac field and zero dc field changing ac frequencies from 1 to 1500 Hz. However, both the in-phase (χ') and out-of-phase (χ'') components of the ac susceptibility of **1** were not frequency-dependent at $T > 1.8$ K. Thus, the measurement was carried out in a 500 Oe dc field. As shown in Figure 7, both χ' and χ'' were frequency-dependent at temperatures below 3 K, suggesting SMM behavior. However, distinct χ'' peaks were not observed above 1.8 K, even at an ac frequency of 1500 Hz.

From the temperature dependence of the ac susceptibilities of **1** in a dc field of 500 Oe in the *T* range of 1.8–2.2 K, shown in Figure 8, an Arrhenius plot was plotted, as shown in Figure 9. The values of τ_0 and Δ_{eff} which were estimated from a least-squares linear fit of $\tau(T) = \tau_0 \exp(\Delta_{\text{eff}}/k_B T)$, were 1.06×10^{-6} s and 14.06 K, respectively. The value of τ_0 is smaller than those of general SMMs (10^{-7} to 10^{-8} s). However, a few examples of SMMs with slow relaxation times ($\sim 10^{-5}$ s) have been reported.⁴⁸ In other words, compound **1** can be regarded as a SMM.

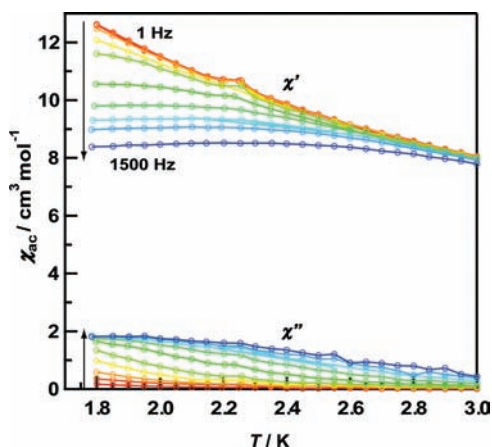


Figure 7. Temperature and frequency dependence of the real (χ') and imaginary (χ'') parts of the ac susceptibility for **1** in 3 Oe ac and 500 Oe dc fields (solid lines are only a guide for the eyes).

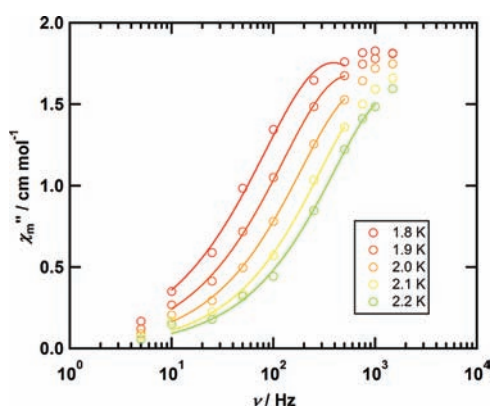


Figure 8. χ'' vs frequency for **1** in the T range of 1.8–2.2 K in a 500 Oe field. Solid lines indicate fitting lines.

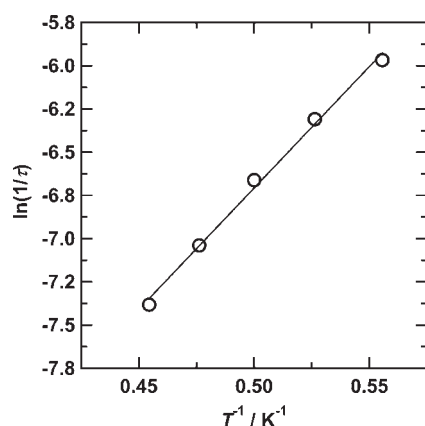


Figure 9. Arrhenius plot of the relaxation times for **1** estimated from the values of χ'' in a dc field of 500 Oe.

4. CONCLUSIONS

The electronic state of a structurally hybridized compound comprised of SMM and conducting layers, $[\text{Mn}(5\text{-MeOsaltmen})(\text{acetone})]_2[\text{Ni}(\text{dmit})_2]_6$, was described. SMM and semiconducting characters coexisted in crystals of **1**, although no correlations

between them could be detected in the conduction and magnetic measurements. These results are similar to those for other hybrid materials, such as $[\text{Mn}(5\text{-MeOsaltmen})(\text{solvent})]_2\text{-}[\text{Ni}(\text{dmit})_2]_7 \cdot 4\text{solvent}$ (solvent = acetone or acetonitrile).²⁴ However, **1** has a much different electronic state than the 2:7 salts have. Compound **1** was determined to be in a charge-ordered state, which should exhibit superconducting or metallic behavior in the conducting layers, although **1** behaved as a band insulator under pressure. Furthermore, the SMM behavior of **1** indicates that the SMM properties can be tuned by changing the combination of SMMs and conducting molecules. Our results represent a new way to prepare hybrid materials based on quantum magnets and molecular conductors.

■ ASSOCIATED CONTENT

S Supporting Information. Energy band structure of **1**. This material is available free of charge via the Internet at <http://pubs.acs.org>.

■ AUTHOR INFORMATION

Corresponding Author

*E-mail: kkubo@es.hokudai.ac.jp (K. K.).

Present Addresses

Research Institute for Electronic Science, Hokkaido University, Kita 20 Nishi 10, Kita-ku, Sapporo 001-0020, Japan. Tel: +81-11-706-9418. Fax: +81-11-706-9420. E-mail: kkubo@es.hokudai.ac.jp (K. K.).

■ ACKNOWLEDGMENT

This work was financially supported by the Young Scientist Encouragement Fund 2009 from the Faculty of Science, Tohoku University and a Grant-in-Aid for Scientific Research from the Ministry of Education, Culture, Sports, Science and Technology, Japan (No. 20850024 and 22224006).

■ REFERENCES

- (a) Coronado, E.; Day, P. *Chem. Rev.* **2004**, *104*, 5419–5448. (b) Enoki, T.; Miyazaki, A. *Chem. Rev.* **2004**, *104*, 5449–5478. (c) Coronado, E.; Galán-Mascarós, J. R. *J. Mater. Chem.* **2005**, *15*, 66–74. (d) Ouahab, L. *Chem. Mater.* **1997**, *9*, 1909–1926.
- (a) Coronado, E.; Galán-Mascarós, J. R.; Gómez-García, C. J.; Laukhin, V. *Nature* **2000**, *408*, 447–449. (b) Alberola, A.; Coronado, E.; Galán-Mascarós, J. R.; Giménez-Saiz, C.; Gómez-García, C. J. *J. Am. Chem. Soc.* **2003**, *125*, 10774–10775.
- (a) Galán-Mascarós, J. R.; Coronado, E.; Goddard, P. A.; Singleton, J.; Coldea, A. I.; Wallis, J. D.; Coles, S. J.; Alberola, A. *J. Am. Chem. Soc.* **2010**, *132*, 9271–9273. (b) Coronado, E.; Martí-Gastaldo, C.; Navarro-Moratalla, E.; Ribera, A.; Blundell, S. J.; Baker, P. *J. Nat. Chem.* **2010**, *2*, 1031–1036.
- (a) Ojima, E.; Fujiwara, H.; Kato, K.; Kobayashi, H.; Tanaka, H.; Kobayashi, A.; Tokumoto, M.; Cassoux, P. *J. Am. Chem. Soc.* **1999**, *121*, 5581–5582. (b) Kurmoo, M.; Graham, A. W.; Day, P.; Coles, S. J.; Hursthouse, M. B.; Caulfield, J. L.; Singleton, J.; Pratt, F. L.; Hayes, W.; Ducas, L.; Guionneau, P. *J. Am. Chem. Soc.* **1995**, *117*, 12209–12227.
- (a) Christou, G.; Gatteschi, D.; Hendrickson, D. N.; Sessoli, R. *MRS Bull.* **2000**, *25*, 66–71. (b) Gatteschi, D.; Sessoli, R. *Angew. Chem., Int. Ed.* **2003**, *42*, 268–297.
- (a) Boyd, P. D. W.; Li, Q.; Vincent, J. B.; Folting, K.; Chang, H.-R.; Streib, W. E.; Huffman, J. C.; Christou, G.; Hendrickson, D. N. *J. Am. Chem. Soc.* **1988**, *110*, 8537–8539. (b) Caneschi, A.; Gatteschi, D.

- Sessoli, R. *J. Am. Chem. Soc.* **1991**, *113*, 5873–5874. (c) Sessoli, R.; Tsai, H.-L.; Schake, A. R.; Wang, S.; Vincent, J. B.; Foltling, K.; Gatteschi, D.; Christou, G.; Hendrickson, D. N. *J. Am. Chem. Soc.* **1993**, *115*, 1804–1816.
- (7) (a) Aubin, S. M. J.; Wemple, M. W.; Adams, D. M.; Tsai, H.; Christou, G.; Hendrickson, D. N. *J. Am. Chem. Soc.* **1996**, *118*, 7746–7754. (b) Yoo, J.; Brechin, E. K.; Yamaguchi, A.; Nakano, M.; Huffman, J. C.; Maniero, A. L.; Brunel, L.-C.; Awaga, K.; Ishimoto, H.; Christou, G.; Hendrickson, D. N. *Inorg. Chem.* **2000**, *39*, 3615–3623. (c) Yoo, J.; Yamaguchi, A.; Nakano, M.; Krzystek, J.; Streib, W. E.; Brunel, L.-C.; Ishimoto, H.; Christou, G.; Hendrickson, D. N. *Inorg. Chem.* **2001**, *40*, 4604–4616. (d) Hendrickson, D. N.; Christou, G.; Ishimoto, H.; Yoo, J.; Brechin, E. K.; Yamaguchi, A.; Rumberger, E. M.; Aubin, S. M. J.; Sun, Z.; Aromi, G. *Polyhedron* **2001**, *20*, 1479–1488. (e) Boskovic, C.; Brechin, E. K.; Streib, W. E.; Foltling, K.; Hendrickson, D. N.; Christou, G. *J. Am. Chem. Soc.* **2002**, *124*, 3725–3736. (f) Brechin, E. K.; Boskovic, C.; Wernsdorfer, W.; Yoo, J.; Yamaguchi, A.; Sanudo, E. C.; Concolino, T.; Rheingold, A. L.; Ishimoto, H.; Hendrickson, D. N.; Christou, G. *J. Am. Chem. Soc.* **2002**, *124*, 9710–9711. (g) Brechin, E. K.; Soler, M.; Davidson, J.; Hendrickson, D. N.; Parsons, S.; Christou, G. *Chem. Commun.* **2002**, 2252–2253.
- (8) (a) Delfs, C.; Gatteschi, D.; Pardi, L.; Sessoli, R.; Wieghardt, K.; Hanke, D. *Inorg. Chem.* **1993**, *32*, 3099–3103. (b) Barra, A. L.; Caneschi, A.; Cornia, A.; Fabrizi de Bianchi, F.; Gatteschi, D.; Sangregorio, C.; Sessoli, R.; Sorace, L. *J. Am. Chem. Soc.* **1999**, *121*, 5302–5310. (c) Gatteschi, D.; Sessoli, R.; Cornia, A. *Chem. Commun.* **2000**, 725–732. (d) Oshio, H.; Hoshino, N.; Ito, T. *J. Am. Chem. Soc.* **2000**, *122*, 12602–12603. (e) Benelli, C.; Cano, J.; Journaux, Y.; Sessoli, R.; Solan, G. A.; Winpenny, R. E. P. *Inorg. Chem.* **2001**, *40*, 188–189. (f) Goodwin, J. C.; Sessoli, R.; Gatteschi, D.; Wernsdorfer, W.; Powell, A. K.; Heath, S. L. *J. Chem. Soc., Dalton Trans.* **2000**, 1835–1840.
- (9) (a) Cadiou, C.; Murrie, M.; Paulsen, C.; Villar, V.; Wernsdorfer, W.; Winpenny, R. E. P. *Chem. Commun.* **2001**, 2666–2667. (b) Andres, H.; Basler, R.; Blake, A. J.; Cadiou, C.; Chaboussant, G.; Grant, C. M.; Güdel, H.-U.; Murrie, M.; Parsons, S.; Paulsen, C.; Semadini, F.; Villar, V.; Wernsdorfer, W.; Winpenny, R. E. P. *Chem.—Eur. J.* **2002**, *8*, 4867–4876. (c) Yang, E.-C.; Wernsdorfer, W.; Hill, S.; Edwards, R. S.; Nakano, M.; Maccagnano, S.; Zakharov, L. N.; Rheingold, A. L.; Christou, G.; Hendrickson, D. N. *Polyhedron* **2003**, *22*, 1727–1733.
- (10) Castro, S. L.; Sun, Z.; Grant, C. M.; Bollinger, J. C.; Hendrickson, D. N.; Christou, G. *J. Am. Chem. Soc.* **1998**, *120*, 2365–2375.
- (11) Yang, E.; Hendrickson, D. N.; Wernsdorfer, W.; Nakano, M.; Zakharov, L. N.; Sommer, R. D.; Rheingold, A. L.; Ledezma-Gairaud, M.; Christou, G. *J. Appl. Phys.* **2002**, *91*, 7382–7388.
- (12) (a) Wernsdorfer, W.; Aliaga-Alcalde, N.; Hendrickson, D. N.; Christou, G. *Nature* **2002**, *416*, 406–409. (b) Tiron, R.; Wernsdorfer, W.; Foguet-Albiol, D.; Aliaga-Alcalde, N.; Christou, G. *Phys. Rev. Lett.* **2003**, *91*, 227203–1–227203–4. (c) Hill, S.; Edwards, R. S.; Aliaga-Alcalde, N.; Christou, G. *Science* **2003**, *302*, 1015–1018. (d) Park, K.; Pederson, M. R.; Richardson, S. L.; Aliaga-Alcalde, N.; Christou, G. *Phys. Rev. B* **2003**, *68*, 020405-1–020405-4. (e) Wernsdorfer, W.; Bhaduri, S.; Tiron, R.; Hendrickson, D. N.; Christou, G. *Phys. Rev. Lett.* **2002**, *89*, 197201–1–197201–4. (f) Edwards, R. S.; Hill, S.; Bhaduri, S.; Aliaga-Alcalde, N.; Bolin, E.; Maccagnano, S.; Christou, G.; Hendrickson, D. N. *Polyhedron* **2003**, *22*, 1911–1916.
- (13) Tiron, R.; Wernsdorfer, W.; Aliaga-Alcalde, N.; Christou, G. *Phys. Rev. B* **2003**, *68*, 140407–1–140407–4.
- (14) Boskovic, C.; Bircher, R.; Tregenna-Piggott, P. L. W.; Güdel, H. U.; Paulsen, C.; Wernsdorfer, W.; Barra, A.-L.; Khatsko, E.; Neels, A.; Stoeckli-Evans, H. *J. Am. Chem. Soc.* **2003**, *125*, 14046–14058.
- (15) Miyasaka, H.; Nakata, K.; Sugiura, K.; Yamashita, M.; Clérac, R. *Angew. Chem., Int. Ed.* **2004**, *43*, 707–711.
- (16) Miyasaka, H.; Nakata, K.; Lecren, L.; Coulon, C.; Nakazawa, Y.; Fujisaki, T.; Sugiura, K.; Yamashita, M.; Clérac, R. *J. Am. Chem. Soc.* **2006**, *128*, 3770–3783.
- (17) Lecren, L.; Roubeau, O.; Coulon, C.; Li, Y.-G.; Le Goff, X. F.; Wernsdorfer, W.; Miyasaka, H.; Clérac, R. *J. Am. Chem. Soc.* **2005**, *127*, 17353–17363.
- (18) Lecren, L.; Wernsdorfer, W.; Li, Y.-G.; Vindigni, A.; Miyasaka, H.; Clérac, R. *J. Am. Chem. Soc.* **2007**, *129*, 5045–5051.
- (19) Miyasaka, H.; Yamashita, M. *Dalton Trans.* **2007**, 399–406.
- (20) (a) Clérac, R.; Miyasaka, H.; Yamashita, M.; Coulon, C. *J. Am. Chem. Soc.* **2002**, *124*, 12837–12844. (b) Miyasaka, H.; Clérac, R.; Mizushima, K.; Sugiura, K.; Yamashita, M.; Wernsdorfer, W.; Coulon, C. *Inorg. Chem.* **2003**, *42*, 8203–8213. (c) Ferbinteanu, M.; Miyasaka, H.; Wernsdorfer, W.; Nakata, K.; Sugiura, K.; Yamashita, M.; Coulon, C.; Clérac, R. *J. Am. Chem. Soc.* **2005**, *127*, 3090–3099. (d) Lecren, L.; Roubeau, O.; Coulon, C.; Li, Y.-G.; Le Goff, X. F.; Wernsdorfer, W.; Miyasaka, H.; Clérac, R. *J. Am. Chem. Soc.* **2005**, *127*, 17353–17363. (e) Miyasaka, H.; Madanbashi, T.; Sugimoto, K.; Nakazawa, Y.; Wernsdorfer, W.; Sugiura, K.; Yamashita, M.; Coulon, C.; Clérac, R. *Chem.—Eur. J.* **2006**, *12*, 7028–7040. (f) Saitoh, A.; Miyasaka, H.; Yamashita, M.; Clérac, R. *J. Mater. Chem.* **2007**, *17*, 2002–2012. (g) Lecren, L.; Roubeau, O.; Li, Y.-G.; Le Goff, X. F.; Miyasaka, H.; Richard, F.; Wernsdorfer, W.; Coulon, C.; Clérac, R. *Dalton Trans.* **2008**, 755–766.
- (21) Hiraga, H.; Miyasaka, H.; Nakata, K.; Kajiwara, T.; Takaishi, S.; Oshima, Y.; Nojiri, H.; Yamashita, M. *Inorg. Chem.* **2007**, *46*, 9661–9671.
- (22) Lecren, L.; Li, Y.-G.; Wernsdorfer, W.; Roubeau, O.; Miyasaka, H.; Clérac, R. *Inorg. Chem. Commun.* **2005**, *8*, 626–630.
- (23) (a) Davison, A.; Edelstein, N.; Holm, R. H.; Maki, A. H. *Inorg. Chem.* **1963**, *2*, 1227. (b) Underhill, A. E.; Ahmad, M. M. *J. Chem. Soc., Chem. Commun.* **1981**, 67–68.
- (24) Hiraga, H.; Miyasaka, H.; Takaishi, S.; Kajiwara, T.; Yamashita, M. *Inorg. Chim. Acta* **2008**, *361*, 3863–3872.
- (25) Hiraga, H.; Miyasaka, H.; Clérac, R.; Fourmigué, M.; Yamashita, M. *Inorg. Chem.* **2009**, *48*, 2887–2898.
- (26) Kato, R. *Chem. Rev.* **2004**, *104*, 5319–5346.
- (27) (a) Shibaeva, R. P.; Yagubskii, E. B. *Chem. Rev.* **2004**, *104*, 5347–5378. (b) Kobayashi, H.; Cui, H.-B.; Kobayashi, A. *Chem. Rev.* **2004**, *104*, 5265–5288.
- (28) Kubo, K.; Miyasaka, H.; Yamashita, M. *Phys. B, Condens. Matter* **2010**, *405*, S313–S316.
- (29) Miyasaka, H.; Clérac, R.; Ishii, T.; Chang, H.-C.; Kitagawa, S.; Yamashita, M. *J. Chem. Soc., Dalton Trans.* **2002**, 1528–1534.
- (30) Steimeche, G.; Sieler, H. J.; Kirmse, R.; Hoyer, E. *Phosphor. Sulfur* **1979**, *7*, 49–55.
- (31) (a) Albright, T. A.; Hofmann, P.; Hoffmann, R. *J. Am. Chem. Soc.* **1977**, *99*, 7546–7557. (b) Joergensen, K. A.; Wheeler, R. A.; Hoffmann, R. *J. Am. Chem. Soc.* **1987**, *109*, 3240–3246. (c) Keszler, D. A.; Hoffmann, R. *J. Am. Chem. Soc.* **1987**, *109*, 118–124.
- (32) Boudreau, E. A.; Mulay, L. N. *Theory and Application of Molecular Paramagnetism*; John Wiley and Sons: New York, 1976; p 491.
- (33) (a) Walker, I. R. *Rev. Sci. Instrum.* **1999**, *70*, 3402–3412. (b) Ishii, Y.; Tamura, M.; Kato, R.; Hedo, M.; Uwatoko, Y.; Mōri, N. *Synth. Met.* **2005**, *152*, 389–393.
- (34) Miyasaka, H.; Clérac, R.; Wernsdorfer, W.; Lecren, L.; Bonhomme, C.; Sugiura, K.-I.; Yamashita, M. *Angew. Chem., Int. Ed.* **2004**, *43*, 2801–2805.
- (35) Faulmann, C.; Delpech, F.; Malfant, I.; Cassoux, P. *J. Chem. Soc., Dalton Trans.* **1996**, 2261–2267.
- (36) Valade, L.; Legros, J.-P.; Bousseau, M.; Cassoux, P.; Garbaskas, M.; Interrante, L. V. *J. Chem. Soc., Dalton Trans.* **1985**, 783–794.
- (37) Nakamura, T.; Underhill, A. E.; Coomber, A. T.; Friend, R. H.; Tajima, H.; Kobayashi, A.; Kobayashi, H. *Inorg. Chem.* **1995**, *34*, 870–876.
- (38) Johannsen, I.; Bechgaard, K.; Rindorf, G.; Thorup, N.; Jacobsen, C. S.; Mortensen, K. *Synth. Met.* **1986**, *15*, 333–343.
- (39) (a) Jérôme, D.; Mazaud, A.; Ribault, M.; Bechgaard, K. *J. Phys., Lett.* **1980**, *41*, 95–98. (b) Creuzet, F.; Jérôme, D.; Moradpour, A. *Mol. Cryst. Liq. Cryst.* **1985**, *119*, 297–302. (c) Jérôme, D. *Science* **1991**, *252*, 1509–1514.
- (40) (a) Taniguchi, H.; Miyashita, M.; Uchiyama, K.; Satoh, K.; Mōri, N.; Okamoto, H.; Miyagawa, K.; Kanoda, K.; Hedo, M.; Uwatoko, Y. *J. Phys. Soc. Jpn.* **2003**, *72*, 468–471. (b) Kini, A. M.; Geiser, U.; Wang, H. H.; Carlson, K. D.; Williams, J. M.; Kwok, W. K.; Vandervoort, K. G.; Thompson, J. E.; Stupka, D. L.; Jung, D.; Whangbo, M.-H. *Inorg. Chem.* **1990**, *29*, 2555–2557. (c) Williams, J. M.; Kini, A. M.; Wang, H. H.;

Carlson, K. D.; Geiser, U.; Montgomery, L. K.; Pyrka, G. J.; Watkins, D. M.; Kommers, J. M.; Boryschuk, S. J.; Crouch, A. V. S.; Kwok, W. K.; Schirber, J. E.; Overmyer, D. L.; Jung, D.; Whangbo, M.-H. *Inorg. Chem.* **1990**, *29*, 3272–3274.

(41) (a) Brossard, L.; Ribault, M.; Valade, L.; Cassoux, P. *Phys. B+C* **1986**, *143*, 313–315. (b) Bousseau, M.; Valade, L.; Legros, J.-P.; Cassoux, P.; Carbauskas, M.; Interrante, L. V. *J. Am. Chem. Soc.* **1986**, *108*, 1908–1916.

(42) (a) Tajima, H.; Yakushi, K.; Kuroda, H.; Saito, G. *Solid State Commun.* **1985**, *56*, 159–163. (b) Jacobsen, C. S.; Tanner, D. B.; Williams, J. M.; Geiser, U.; Wang, H. H. *Phys. Rev. B* **1987**, *35*, 9605–9613.

(43) (a) Pokhodnya, K. I.; Cassoux, P.; Feltre, L.; Meneghetti, M. *Synth. Met.* **1999**, *103*, 2187. (b) Romaniello, P.; Lelj, F.; Arca, M.; Devillanova, F. A. *Theor. Chem. Acc.* **2007**, *117*, 621–635.

(44) Yamamoto, T.; Nakazawa, Y.; Tamura, M.; Fukunaga, T.; Kato, R.; Yakushi, K. *Phys. J. Phys. Soc. Jpn.* **2011**, *80*, 074717–1–074717–16.

(45) Miyagawa, K.; Kanoda, K.; Kawamoto, A. *Chem. Rev.* **2004**, *104*, 5635–5654.

(46) Thomas, L.; Lioni, F.; Ballou, R.; Gatteschi, D.; Sessoli, R.; Barbara, B. *Nature* **1996**, *383*, 145–147.

(47) (a) Ako, A. M.; Mereacre, V.; Hewitt, I. J.; Clérac, R.; Lecren, L.; Anson, C. E.; Powell, A. K. *J. Mater. Chem.* **2006**, *16*, 2579–2586. (b) Kachi-Terajima, C.; Miyasaka, H.; Saitoh, A.; Shirakawa, N.; Yamashita, M.; Clérac, R. *Inorg. Chem.* **2007**, *46*, 5861–5872.

(48) (a) Ishikawa, N.; Sugita, M.; Ishikawa, T.; Koshihara, S.; Kaizu, Y. *J. Am. Chem. Soc.* **2003**, *125*, 8694–8695. (b) Boskovic, C.; Bircher, R.; Tregenna-Piggott, P. L. W.; Güdel, H. U.; Paulsen, C.; Wernsdorfer, W.; Barra, A.-L.; Khatsko, E.; Neels, A.; Stoeckli-Evans, H. *J. Am. Chem. Soc.* **2003**, *125*, 14046–14058. (c) Gatteschi, D.; Sessoli, R.; Cornia, A. *Chem. Commun.* **2000**, 725–732.

(49) A conducting single-molecule magnet based on the Mn-salen dimer and Ni(dmit)₂ complexes was obtained by electrochemical crystallization and was characterized by elemental and crystallographic analyses, band calculations, and electrical resistivity and magnetic susceptibility measurements.